A physically motivated sparse cubature scheme with applications to molecular density-functional theory

2008 J. Phys. A: Math. Theor. 41 365202

(http://iopscience.iop.org/1751-8121/41/36/365202)

IOP PUBLISHING JOURNAL OF PHYSICS A: MATHEMATICAL AND THEORETICAL

J. Phys. A: Math. Theor. **41** (2008) 365202 (18pp) doi:10.1088/1751-8113/41/36/365202

A physically motivated sparse cubature scheme with applications to molecular density-functional theory

Juan I Rodriguez[1], David C Thompson[1,2], James S M Anderson[1], Jordan W Thomson[1] and Paul W Ayers[1]

[1] Department of Chemistry, McMaster University, Hamilton, Ontario L8S 4M1, Canada
[2] Boehringer Ingelheim Pharmaceuticals, Inc., 900 Ridgebury Road, Ridgefield, CT 06877, USA

Received 29 March 2008, in final form 18 June 2008
Published 30 July 2008
Online at stacks.iop.org/JPhysA/41/365202

Abstract

We present a novel approach for performing multi-dimensional integration of arbitrary functions. The method starts with Smolyak-type sparse grids as cubature formulae on the unit cube and uses a transformation of coordinates based on the conditional distribution method to adapt those formulae to real space. Our method is tested on integrals in one, two, three and six dimensions. The three dimensional integration formulae are used to evaluate atomic interaction energies via the Gordon–Kim model. The six dimensional integration formulae are tested in conjunction with the nonlocal exchange-correlation energy functional proposed by Lee and Parr. This methodology is versatile and powerful; we contemplate application to frozen-density embedding, next-generation molecular-mechanics force fields, 'kernel-type' exchange-correlation energy functionals and pair-density functional theory.

PACS number: 31.15.E−

1. Introduction

One of the most pervasive tasks in modern computational simulation is numerical integration. This is especially true in many-body quantum mechanics, where the integrals that need to be performed often have high dimensionality and where the integrands are often strongly inhomogeneous. Consider, for example, that in order to attain so-called 'chemical accuracy' for a molecular system (i.e., enough accuracy in an energy calculation to predict the rate of a chemical reaction to within an order of magnitude), one often has to integrate strongly peaked functions very accurately, with relative errors of less than 0.001%. (For moderate-sized molecules, the 'chemically relevant' portion of the electron density spans five to seven orders of magnitude.) Such daunting integration tasks would be manifestly impossible were it not for the ability of physicists and chemists to 'guess' the structure of the integrand based on mathematical conditions and physicochemical insight. The goal of this paper is to introduce

a general approach that leverages prior knowledge about the integrands to design an efficient numerical integration method.

In particular, we will introduce a universally applicable method for performing d-dimensional integrals,

$$\int_{\mathbb{R}^d} f(\mathbf{r}) P(\mathbf{r}) \, \mathrm{d}r \approx \sum_{i=1}^{M_L} w_i f(\mathbf{r}_i), \tag{1}$$

where $P(\mathbf{r}) > 0$ is any non-negative integrable 'weight function'. This form of integration allows one to leverage most of one's knowledge about the integrand of interest. In particular, one can ensure that $f(\mathbf{r})$ is smooth by ensuring that the analytically defined $P(\mathbf{r})$ correctly models all of the singularities and nondifferentiability of the integrand. (In molecular-electronic structure calculations, for example, $P(\mathbf{r})$ should model the electron-nuclear cusps in the electron density/wavefunction [1–7].) Ideally, $P(\mathbf{r})$ should be chosen so that $f(\mathbf{r})$ is slowly varying. To the extent that this cannot be achieved, then $P(\mathbf{r})$ should be largest in the regions where $f(\mathbf{r})$ varies most strongly. In this way, knowledge of the structure of the integrand allows us to construct more efficient quadrature methods.

But what numerical methods should we use to perform these integrals? In one dimension, the answer is clear: Gaussian quadrature formulae with respect to the weight function, $P(x)$, will be the optimal integration method [8–11]. Similarly, Gaussian cubature would be optimal in higher dimensions. However, constructing even low-order Gaussian cubature formulae is very difficult and time consuming; such methods are clearly inappropriate given the large number (usually hundreds, sometimes millions) of integrals required in molecular electronic structure theory calculations, which is the application of greatest interest to us. (Hall and Rees have done work on Gaussian cubature formulae for atoms [12] and homonuclear diatomic molecules [13], but their approach seems daunting even for these systems, and it is not clear whether it can be extended to large molecules. Moreover, it does not seem easy to apply their method to arbitrary choices for $P(\mathbf{r})$.)

While Gaussian cubature formulae are not known for arbitrary choices of $P(\mathbf{r})$, Gaussian cubature formulae are known for certain special integration regions and certain special weight functions, e.g., the uniformly weighted unit cube. Even when Gaussian cubature formulae are not known for a region, other efficient formulae are [14–16]. The approach we will take uses one of these 'almost as good' cubature formulae for the unit cube, due to Smolyak [17]. After that cubature formula has been defined on the unit cube, we will transform it to real space using a transformation whose Jacobian determinant is $P(\mathbf{r})$, thereby obtaining an efficient cubature formula for integrals with the form of equation (1). The mathematical details of the procedure are presented in the following section, followed by the results of our numerical tests. We conclude with a short summary of our findings and a brief prospectus for future work.

2. Method

2.1. One-dimensional quadrature grids on [0, 1]

It is commonly asserted that, for smooth functions in one dimension, the best numerical integration formulae are the Gaussian quadrature formulae. There are many different ways to explain why the Gaussian quadrature formulae are 'best', but one of the most useful is through a discussion of their computational complexity. The computational complexity, $C(\varepsilon)$, is the

computational cost required to achieve accuracy, ε [18, 19]. The integration error when an n-point Gaussian quadrature formula is applied to an r-times differentiable function is

$$\varepsilon \sim n^{-r}. \tag{2}$$

The computational cost is proportional to the number of times the function has to be evaluated, n. So

$$C_{\mathrm{Ga}}(\varepsilon) \sim \varepsilon^{-1/r}. \tag{3}$$

These formulae may be derived from the asymptotic decay of the coefficients of the orthogonal polynomials that underlie the Gaussian quadrature formulae and from the defining property of Gaussian quadrature: the n-point Gaussian quadrature formula exactly integrates all of the associated orthogonal polynomials of degree $2n-1$ or less [9, 11, 20]. It is important to note that these results are asymptotic: they only hold in the high-accuracy (large n, small ε) limit. When lower accuracy suffices, alternative numerical integration techniques may be preferable.

Gaussian quadrature is 'optimal' because the results in equations (2) and (3) are optimal. Other common formulae are less efficient. For comparison, the computational complexity of the Monte Carlo integration, the trapezoidal rule and Simpson's rule are $C_{\mathrm{MC}}(\varepsilon) \sim \varepsilon^{-2}$, $C_{\mathrm{Tr}}(\varepsilon) \sim \varepsilon^{-1/2}$ and $C_{\mathrm{Si}}(\varepsilon) \sim \varepsilon^{-1/4}$, respectively, for sufficiently smooth integrands. There are other one-dimensional quadrature formulae that approach the utility of the Gauss formulae; the Clenshaw–Curtis formula is competitive with Gaussian quadrature [21, 22]. For periodic integrands, the trapezoidal rule is a 'trigonometric' Gaussian quadrature formula; in that context the trapezoidal rule is usually referred to as the rectangle rule. In the quantum chemistry community, the rectangle rule is usually referred to as the Euler–MacLaurin formula [23]. Both the rectangle rule and the Clenshaw–Curtis rule are nested quadratures: points from the lower order quadratures are reused in higher order formulae. Because nested grids are numerically advantageous for our application and the rectangle and Clenshaw–Curtis rules have 'near-Gaussian' quality, we will consider only these rules in this paper. Moreover, we are primarily interested in quadrature formulae on the unit interval,

$$\int_0^1 f(x)\,\mathrm{d}x \approx Q_l[f] \equiv \sum_{i=1}^{m_l} w_i f(x_i). \tag{4}$$

Here, l denotes the order of the quadrature formula, m_l denotes the number of points in the formula, x_i are the grid points in the formula and w_i are the weights.

2.2. Multi-dimensional grids on [0, 1]^d

Numerical integration in many dimensions is intrinsically more difficult than one-dimensional integration. The error and computational complexity for integrating an r-times differentiable d-dimensional function is

$$\varepsilon \sim n^{-r/d} \qquad C(\varepsilon) \sim \varepsilon^{-d/r}. \tag{5}$$

The complexity of numerical integration grows exponentially with increasing dimension; this is often referred to as the 'curse of dimension'.

It is possible to break the curse of dimension when the function is more than 'just' differentiable. For example, suppose the integrand has mixed derivatives of order r,

$$\left| \frac{\partial^{n_1}\partial^{n_2}\cdots\partial^{n_d} f(x_1, x_2, \ldots, x_d)}{\partial x_1^{n_1}\partial x_2^{n_2}\cdots\partial x_d^{n_d}} \right| < \infty, \qquad n_1, n_2, \ldots, n_d \leqslant r. \tag{6}$$

This function is more than 'just r-times differentiable' because certain special higher order derivatives exist, so long as none of the variables is differentiated with respect to more than

r times. The integration error and computational complexity for functions with bounded mixed derivatives of order r no longer depends on the dimension. In fact, the computational complexity is now the same as one-dimensional Gaussian quadrature,

$$C_{\text{Mixed}}(\varepsilon) \sim \varepsilon^{-1/r}. \tag{7}$$

This optimal computational complexity is achieved by Gaussian cubature formulae.

Unfortunately, Gaussian cubature formulae are very difficult to construct. Indeed, one has replaced a very difficult problem (integration in higher dimensions) with another one (determining optimal integration formulae) [24]. Instead, one usually constructs higher dimensional formulae as the tensor product of the one-dimensional Gaussian quadrature formulae,

$$\begin{aligned} Q^{(d)}_{l_1 l_2 \cdots l_d}[f] &= Q_{l_1} \otimes Q_{l_2} \otimes \cdots \otimes Q_{l_d}[f] \\ &= \sum_{i_1=1}^{m_{l_1}} \sum_{i_2=1}^{m_{l_2}} \cdots \sum_{i_d=1}^{m_{l_d}} w_{i_1} w_{i_2} \cdots w_{i_d} f\left(x_{i_1}, x_{i_2}, \ldots, x_{i_d}\right). \end{aligned} \tag{8}$$

The very commonly used simple-product cubature formula, $Q^{(L,d)}_{\text{SP}}[f] = Q^{(d)}_{l_1=l_2=\cdots=l_d=L}[f]$, occurs when one integrates in each dimension using the same one-dimensional formula. The complexity of the simple-product formula is

$$C_{\text{SP}}(\varepsilon) \sim \varepsilon^{-d/r}. \tag{9}$$

The simple-product rule is optimal for functions that are merely differentiable, but is exponentially suboptimal for functions with bounded mixed derivatives.

One can do much better than the simple-product rule by considering a linear combination of simple-product formulae with different orders. In this paper we will focus on the Smolyak rule [17]:

$$\begin{aligned} Q^{(L,d)}_{\text{Sm}}[f] &= \sum_{L-d+1 \leqslant |\mathbf{l}|_1 \leqslant L} (-1)^{L-|\mathbf{l}|_1} \binom{d-1}{q-|\mathbf{l}|_1} Q^{(d)}_{l_1 l_2 \cdots l_d}[f] \\ |\mathbf{l}|_1 &= l_1 + l_2 + \cdots + l_d. \end{aligned} \tag{10}$$

The Smolyak rule is within a logarithmic factor of the optimal computational complexity for both differentiable functions (equation (5)) and for mixed-differentiable functions (equation (7)) [25, 26]. The Smolyak rule is not optimal, but more efficient formulae are significantly more difficult to understand and implement [27, 28]. There has been some formal mathematical work [29–31] and proof-of-principle applications of the Smolyak method to the quantum theory of electronic structure [32–34]. Additional details can be found in the review article by Bungartz and Griebel [35].

Most of the previous work on the Smolyak rule has focused on integration over hypercubes,

$$\int_0^1 \cdots \int_0^1 \int_0^1 f(x_1, x_2, \ldots, x_d)\, \mathrm{d}x_1\, \mathrm{d}x_2 \cdots \mathrm{d}x_d \approx Q^{(L,d)}_{\text{Sm}}[f] = \sum_{i=1}^{M_L} w_i f(\mathbf{x}_i). \tag{11}$$

The Smolyak rule for hypercubes can be constructed from any one-dimensional quadrature formula on [0, 1]. Our work was guided by that of Novak and Ritter, who have implemented and tested the Smolyak rule built from the one-dimensional Clenshaw–Curtis formula [36] and the one-dimensional rectangle rule [37]. Figure 1 shows the distribution of points in the two-dimensional Smolyak-rectangle rule (figure 1(*a*)) and the Smolyak–Clenshaw–Curtis rule (figure 1(*b*)). Note that the Smolyak grids are just simple-product grids in which most of the points have been pruned away, with the points that remain reweighted accordingly. This can

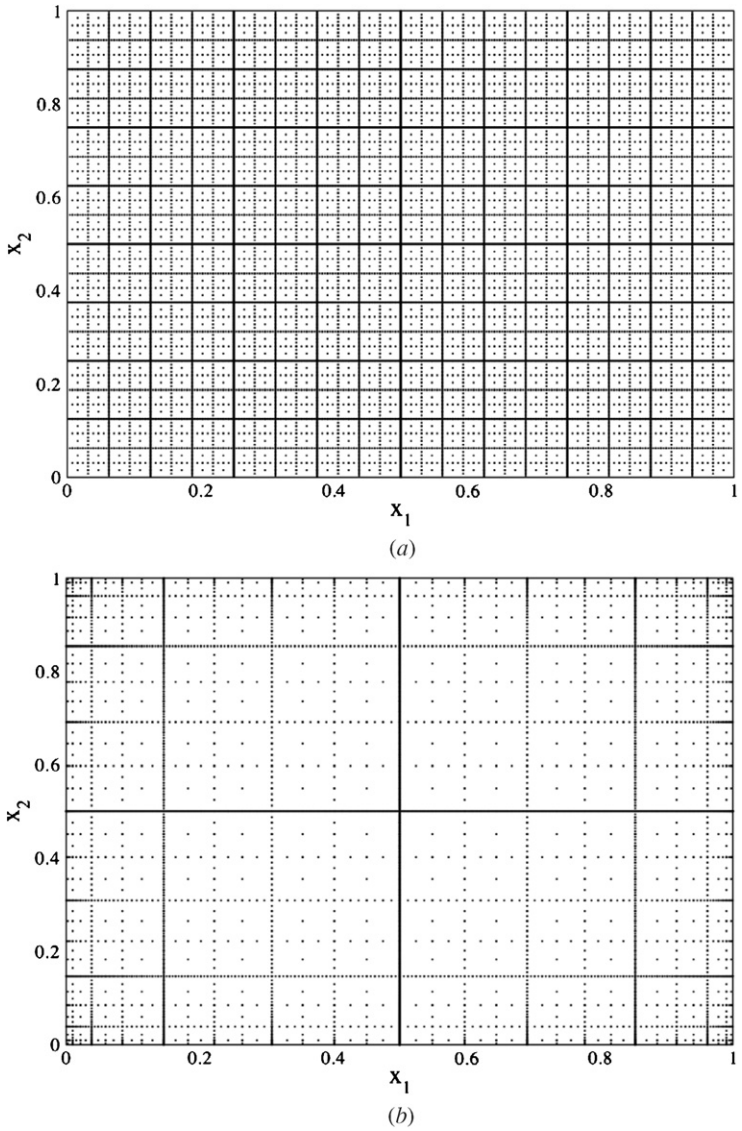

Figure 1. The location of the points in the 11th-order two-dimensional Smolyak grids for (*a*) the rectangle rule and (*b*) the Clenshaw–Curtis rule.

be done because for functions with bounded mixed derivatives, knowing the detailed behavior of the function in certain regions (e.g., along the central lines in the grid) is sufficient to determine the behavior nearby.

Table 1 lists the number of grid points in the Smolyak-rectangle rule and the Smolyak–Clenshaw–Curtis rule for different dimensions. The number of grid points in the simple-product rectangle rule is listed for comparison. Even though the Smolyak cubatures have many fewer points than the simple-product cubatures, the approaches have the same order of accuracy. Smolyak cubatures are far superior to simple-product grids for molecular problems [34].

Table 1. The number of points, M_L, in the Smolyak integration grid of order L built from the one-dimensional rectangle rule (RR) and the Clenshaw–Curtis rule (CC). For comparison, the number of points in a simple-product grid (SP) based on the rectangle rule is also included. Points on the boundary of the hypercube are not counted in this tabulation because they are mapped to infinity by the conditional distribution transformation, equation (13).

	One dimension		Two dimensions			Three dimensions			Six dimensions		
L	RR	CC	RR	CC	SP	RR	CC	SP	RR	CC	SP
1	1	1	1	1	1	1	1	1	1	1	1
2	3	1	5	1	9	7	1	27	13	1	729
3	7	3	17	5	49	31	7	343	97	13	117 649
4	15	7	49	13	225	111	19	3375	545	37	1.1×10^7
5	31	15	129	33	961	351	55	29 791	2561	145	8.9×10^8
6	63	31	321	81	3969	1023	151	2.5×10^5	10 625	481	6.3×10^{10}
7	127	63	769	193	16 129	2815	399	2.0×10^6	40 193	1553	4.2×10^{12}
8	255	127	1793	449	65 025	7423	1023	1.7×10^7	1.4×10^5	4817	2.7×10^{14}
9	511	255	4097	1025	2.6×10^5	18 943	2559	1.3×10^8	4.7×10^5	14 465	1.8×10^{16}
10	1023	511	9217	2305	1.0×10^6	47 103	6271	1.1×10^9	1.5×10^6	42 241	1.1×10^{18}

2.3. The conditional distribution transformation to $(-\infty,\infty)^d$

The Smolyak rule provides an accurate integration grid for the cube, $[0, 1]^d$. However, we are primarily interested in weighted integrals over all space, equation (1). We will use the conditional distribution method [38–41] to define an appropriate transformation of coordinates. Specifically, we define a coordinate transformation

$$\mathbf{x} \in [0, 1]^d \leftrightarrow \mathbf{R} \in (-\infty, \infty)^d \tag{12}$$

with

$$\begin{aligned}
x_1(R_1) &= \frac{\int_{-\infty}^{R_1}\int_{-\infty}^{\infty}\cdots\int_{-\infty}^{\infty} P(r_1, r_2, \ldots, r_d)\,\mathrm{d}r_d\cdots\mathrm{d}r_2\,\mathrm{d}r_1}{\int_{-\infty}^{\infty}\int_{-\infty}^{\infty}\cdots\int_{-\infty}^{\infty} P(r_1, r_2, \ldots, r_d)\,\mathrm{d}r_d\cdots\mathrm{d}r_2\,\mathrm{d}r_1},\\
x_2(R_1, R_2) &= \frac{\int_{-\infty}^{R_2}\int_{-\infty}^{\infty}\cdots\int_{-\infty}^{\infty} P(R_1, r_2, r_3, \ldots, r_d)\,\mathrm{d}r_d\cdots\mathrm{d}r_3\,\mathrm{d}r_2}{\int_{-\infty}^{\infty}\int_{-\infty}^{\infty}\cdots\int_{-\infty}^{\infty} P(R_1, r_2, r_3, \ldots, r_d)\,\mathrm{d}r_d\cdots\mathrm{d}r_3\,\mathrm{d}r_2},\\
&\vdots\\
x_d(R_1, R_2, \ldots, R_d) &= \frac{\int_{-\infty}^{R_d} P(R_1, R_2, \ldots, R_{d-1}, r_d)\,\mathrm{d}r_d}{\int_{-\infty}^{\infty} P(R_1, R_2, \ldots, R_{d-1}, r_d)\,\mathrm{d}r_d}.
\end{aligned} \tag{13}$$

The transformation is one-to-one as long as $P(\mathbf{R})$ is positive, and the transformation exists as long as all of the integrals in equation (13) exist. (For practical purposes, it is helpful if the integrals have simple and explicit analytical expressions.)

The Jacobian determinant for this transformation is

$$|\mathbf{J}| = \frac{P(\mathbf{R})}{\int_{-\infty}^{\infty}\int_{-\infty}^{\infty}\cdots\int_{-\infty}^{\infty} P(\mathbf{r})\,\mathrm{d}\mathbf{r}} \tag{14}$$

and so the cubature rule on the unit cube, equation (11), can be rewritten as a rule for weighted integrals in real space

$$\int_{-\infty}^{\infty}\int_{-\infty}^{\infty}\cdots\int_{-\infty}^{\infty} g(\mathbf{R})P(\mathbf{R})\,\mathrm{d}\mathbf{r} \approx \left(\sum_{i=1}^{M_L} w_i g(\mathbf{R}(\mathbf{x}_i))\right) \times \int_{-\infty}^{\infty}\int_{-\infty}^{\infty}\cdots\int_{-\infty}^{\infty} P(\mathbf{R})\,\mathrm{d}\mathbf{R}. \tag{15}$$

The points in the real-space grid, $\mathbf{R}(\mathbf{x}_i)$, are determined using the inverse of the coordinate transformation in equation (13).

Note that this transformation can be used for any integration grid on $[0, 1]^d$. In this paper, we will use the transformation for the Smolyak rule, but if better choices were available, one could use those grids. For example, Gaussian cubature formulae for the three-dimensional cube are known when the number of points is small, and would be a good choice when a small number of grid points will suffice [14–16]. Perez-Jorda previously applied the conditional-distribution transformation to the simple-product grid, $Q_{\mathrm{SP}}^{(d)}$ [42].

A few of the noteworthy features of this transformation follow.

(1) The transformed grid points are concentrated in regions where $P(\mathbf{R})$ is large and depleted in regions where $P(\mathbf{R})$ is small. In fact, for uniformly distributed points, the probability of observing a point at $\mathbf{R}$ is precisely $P(\mathbf{R})$. This property is exploited in some other applications, where the conditional-distribution transformation is used for random-number generation with respect to the distribution $P(\mathbf{R})$ [38].

(2) Points on the boundaries of the cube are transformed to $\pm\infty$. For this reason, it is important to ensure that the integrand in equation (15) decays faster than $P(\mathbf{R})$ asymptotically (i.e., $g(\mathbf{R})$ needs to decay to zero asymptotically). This is inconvenient because it requires careful selection of the weight function, but it is advantageous because neglecting the boundary points reduces the number of grid points. Both the rectangle rule and the Clenshaw–Curtis rule have points on the boundary of the interval. Those points are not counted in the tabulation of points in table 1.

(3) The transformation of coordinates can be performed rapidly if the partial indefinite integrals of $P(\mathbf{R})$ in equation (13) can be performed analytically. In our work, we use fits of $P(\mathbf{R})$ to Gaussian-type functions,

$$P(\mathbf{R}) = \sum_{\alpha}\sum_{i} c_{\alpha i}\,\mathrm{e}^{-a_{\alpha i}|\mathbf{R}-\mathbf{R}_\alpha|^2}. \tag{16}$$

This choice is motivated by the prevalence of Gaussian-type functions in computational models of molecular electronic structure [43–45].

(4) If the grid points in the hypercube are invariant with respect to 180° rotation about the axis $x_i = \frac{1}{2}$ and $P(\mathbf{R})$ is invariant with respect to 180° rotation about $R_i = 0$, then the transformed grid points will also be invariant with respect to 180° rotation about $R_i = 0$. 90° rotations about the Cartesian axes are similarly preserved, but other symmetries in $P(\mathbf{R})$ (rotations about the non-Cartesian axes, 120° rotations, etc) are not generally maintained because those symmetries are absent from the underlying hypercube.

(5) Integration formulae for irregular integration regions can be obtained by choosing $P(\mathbf{R}) = 0$ outside the region of interest. The transformation is no longer one-to-one and so the integration formulae may not be unique (though they will usually be). However, if $P(\mathbf{R})$ is continuous, then all of the integration formulae are equivalent.

The selection of an appropriate $P(\mathbf{R})$ will differ from application to application. We are primarily interested in applications to molecular electronic structure; in this field, the integrands tend to be the largest in regions where the probability of observing an electron is the greatest (because these regions contribute the largest amount to molecular properties).

This suggests that it will often be fruitful to choose $P(\mathbf{R})$ to be the electron density of the molecule of interest. In general, the electron density is not known until *after* the calculation is complete, however, so one needs to approximate it. For this purpose we will choose the promolecular density [46]: the sum of the densities of the atoms the molecule comprises, centered at the positions of the associated atomic nucleus,

$$P(\mathbf{R}) = \rho_{\text{pro}}(\mathbf{R}) = \sum_{\alpha=1}^{N_{\text{atoms}}} \rho_\alpha(\mathbf{R} - \mathbf{R}_\alpha) \approx \rho(\mathbf{R}). \tag{17}$$

Note that the promolecular electron density will take the convenient form in equation (16) if each atomic density is expressed as a sum of Gaussian-type functions. Constans and Carbó have fit the atomic densities from accurate Hartree–Fock calculations to Gaussians; we will use their fits in this paper [45].

For the purpose of illustration, consider the two-dimensional H_4 molecule, with four pseudo-hydrogen atoms with densities $\rho_{\text{H}}(x_1, x_2) = \frac{2}{\pi}\,\mathrm{e}^{-2\sqrt{x_1^2+x_2^2}}$ centered at $(\pm 1, \pm 1, 0)$. (Distances are measured in atomic units.) The points in the transformed Smolyak grids corresponding to this 'molecule' are shown in figures 2(*a*) (rectangle rule) and (*b*) (Clenshaw–Curtis rule). Note that the points are concentrated in the regions where the atomic density is the largest (near the atoms) and depleted in regions where the electron density is small.

When the integrand does not resemble $P(\mathbf{R})$, this provides a stringent test for the quality of the grids. Figure 3 shows the results obtained by using the pseudo-H_4 grid to integrate a simple Gaussian function,

$$\pi = \int_{-\infty}^{\infty}\int_{-\infty}^{\infty} \mathrm{e}^{-x_1^2-x_2^2}\,\mathrm{d}x_1\,\mathrm{d}x_2. \tag{18}$$

As the number of points in the Smolyak grids increases, the results of the integration rapidly converge to the correct value.

3. Results

3.1. Gaussian function

To provide a more realistic test of the convergence of the Smolyak formulae, figure 4 presents the results for the convergence for an integrand that is a Gaussian,

$$f(x_1, x_2, \ldots, x_d) = \prod_{i=1}^{d} \exp\left(-(d-i+1)x_i^2\right) = \exp\left(-x_d^2 - 2x_{d-1}^2 - 3x_{d-2}^2 - \cdots\right), \tag{19}$$

with respect to a weight that is also a Gaussian,

$$P(x_1, x_2, \ldots, x_d) = \prod_{i=1}^{d} \exp\left(-\tfrac{1}{2}x_i^2\right). \tag{20}$$

Note that the Gaussian weight decays significantly more slowly than the integrand; this is required because we are ignoring boundary points.

Referring to figure 4, the rectangle rule seems to be much better than the Clenshaw–Curtis rule. This may be explained by the tendency for the Clenshaw–Curtis rule to 'bunch up points' near the edges of the integration interval (see figure 1(*b*)). This is advantageous when the function does not behave well near the boundary of the interval, but the function we are

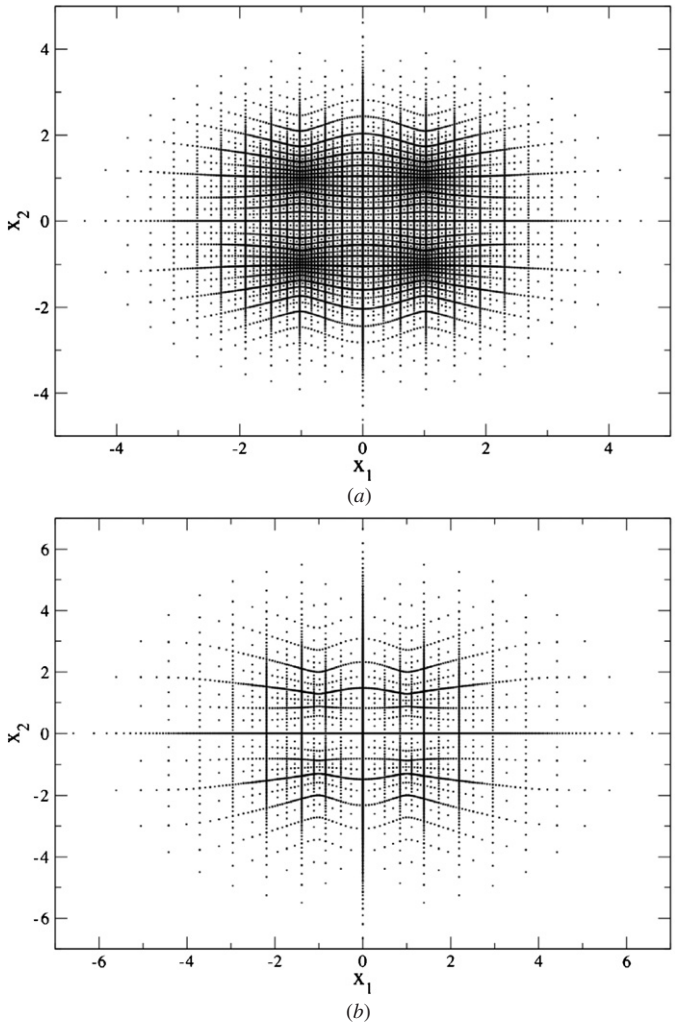

Figure 2. The location of the points in the transformed 11th-order Smolyak grid for the two-dimensional 'pseudo-H_4' molecule with atoms located at $(\pm 1, \pm 1)$. (*a*) The transformed Smolyak-rectangle rule from figure 1(*a*). (*b*) The transformed Smolyak–Clenshaw–Curtis rule from figure 1(*b*).

integrating here decays exponentially quickly asymptotically. The rectangle rule, which has a higher concentration of points in the center of the interval, performs much better for this sort of integral. We also observed that the rectangle rule formulae seem less prone to round-off error than the Clenshaw–Curtis formulae.

3.2. The Gordon–Kim model

Heartened by the results obtained from this simple test, we decided to explore the efficiency of the transformed Smolyak integration grids for the types of integrals that appear in density-functional theory. Our first test uses the simple density-functional theory model of molecular interactions proposed by Gordon and Kim [47]. In this model, the interaction potential between

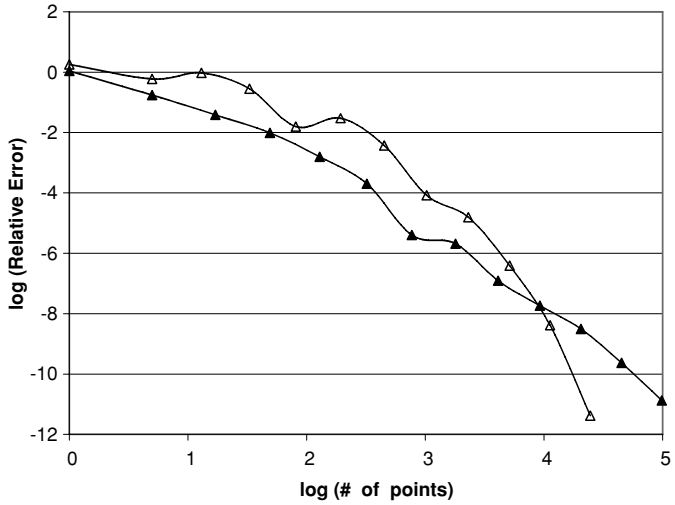

Figure 3. The convergence of the Smolyak formulae for the integral of a two-dimensional Gaussian, equation (18), using the pseudo-H_4 grid shown in figure 2. The $\log_{10}$(relative error) rapidly decreases as $\log_{10}$(number of grid points) increases. Results for the rectangle rule are reported using closed symbols (—▲—) and results for the Clenshaw–Curtis rule are reported using open symbols (—△—).

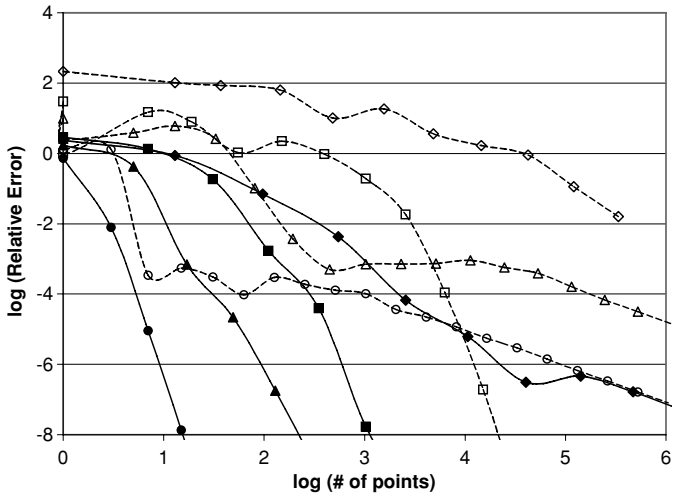

Figure 4. The convergence of the Smolyak formulae for integrating the Gaussian in equation (19) using the weight function given in equation (20). The plot shows $\log_{10}$(relative error) versus $\log_{10}$(number of grid points). The rectangle rule results are denoted by: one dimension (—●—); two dimensions (—▲—); three dimensions (—■—); six dimensions (—◆—). The results for the Clenshaw–Curtis rule are denoted with the analogous open symbols.

two atoms, one of which (denoted α) is centered at the origin and the other (denoted β) is centered R atomic units away, is approximated as

$$V_{\alpha\beta}(R) = \frac{Z_\alpha Z_\beta}{R} + \int\int \frac{\rho_\alpha(\mathbf{r})\rho_\beta(\mathbf{r}')}{|\mathbf{r}-\mathbf{r}'|}\,\mathrm{d}\mathbf{r}\,\mathrm{d}\mathbf{r}' - \int \frac{Z_\alpha \rho_\alpha(\mathbf{r})}{r}\,\mathrm{d}\mathbf{r} - \int \frac{Z_\beta \rho_\beta(\mathbf{r})}{|\mathbf{r}-[0,0,R]|}\,\mathrm{d}\mathbf{r} + T_s^{(\text{non-add})}[\rho_\alpha, \rho_\beta] + E_x^{(\text{non-add})}[\rho_\alpha, \rho_\beta] + E_c^{(\text{non-add})}[\rho_\alpha, \rho_\beta]. \quad (21)$$

In this equation, the electron density for atom α, $\rho_\alpha(\mathbf{r})$, is centered on the origin; the electron density for atom β is centered on the z-axis, R units away. The first four terms in equation (21) are just the electrostatic interactions between the nuclei, between the electron densities of the isolated atoms and between the electron densities of each atom with the other nucleus. These terms capture the electrostatic contribution to binding in the 'frozen density approximation'. The frozen density approximation is accurate when the atoms are so far apart that their electron densities are not significantly polarized.

The last three terms in equation (21) are the non-additive contributions to the kinetic energy, exchange energy and correlation energy, respectively; these are defined by subtracting the value of the function for the molecule from the value of the functional for the atoms,

$$Q^{(\text{non-add})}[\rho_\alpha, \rho_\beta] \equiv Q[\rho_\alpha + \rho_\beta] - Q[\rho_\alpha] - Q[\rho_\beta]. \tag{22}$$

The non-additive contributions are usually evaluated using explicit Thomas–Fermi-like functionals. Here we have elected to use the Thomas–Fermi kinetic energy functional [48, 49]

$$T_s^{\text{TF}}[\rho] = \frac{3(3\pi^2)^{2/3}}{10} \int \rho^{5/3}(\mathbf{r})\, \mathrm{d}\mathbf{r}, \tag{23}$$

the McWeeny reparameterization [50] of the Wigner correlation functional [51]

$$E_c^{\text{MW}}[\rho] = -\int \frac{\rho^{4/3}(\mathbf{r})}{2.946 + 9.652\rho^{1/3}(\mathbf{r})}\, \mathrm{d}\mathbf{r}, \tag{24}$$

and the Dirac exchange functional [52–54] with the Rae [55, 56] self-interaction correction [57] factor,

$$E_x^{\text{RD}}[\rho] = -\kappa(N) \left(\frac{3}{4} \left(\frac{3}{\pi} \right)^{1/3} \right) \int \rho^{4/3}(\mathbf{r})\, \mathrm{d}\mathbf{r}. \tag{25}$$

Here, N denotes the number of electrons. Rae's correction factor is obtained by solving the equation [55, 56]

$$1 = N\delta^3(\delta^3 - 4.5\delta + 4) \tag{26}$$

and then computing

$$\kappa(N) = 1 - \tfrac{8}{3}\delta + 2\delta^2 - \tfrac{1}{3}\delta^3. \tag{27}$$

To evaluate the Gordon–Kim expression for the interaction energy, we need an accurate expression for the ground-state electron densities of the isolated atoms. We have again used the Gaussian atomic density fits of Constans and Carbó [45],

$$\rho_\alpha(\mathbf{r}) = \sum_i c_{\alpha i}\, \mathrm{e}^{-a_{\alpha i} r^2}. \tag{28}$$

One advantage of this form is that the electrostatic contributions to the energy can be evaluated analytically, so only the non-additive terms in equation (21) require numerical integration. While the Constans–Carbó fits are not accurate enough for truly quantitative results, they are certainly sufficient for testing our integration techniques.

The last three terms in equation (21) need to be evaluated numerically. To do this, we construct the promolecular density (cf equation (17)) from the Constans–Carbó densities and, as described in section 2.3, use this as the weight function for the conditional distribution transformation. Since the promolecular density depends on the position of the atoms, the transformed-Smolyak grids adapt to changes in the internuclear distance by placing more points in regions where the density is the highest (near the atomic nuclei) and fewer points far from the atomic nuclei.

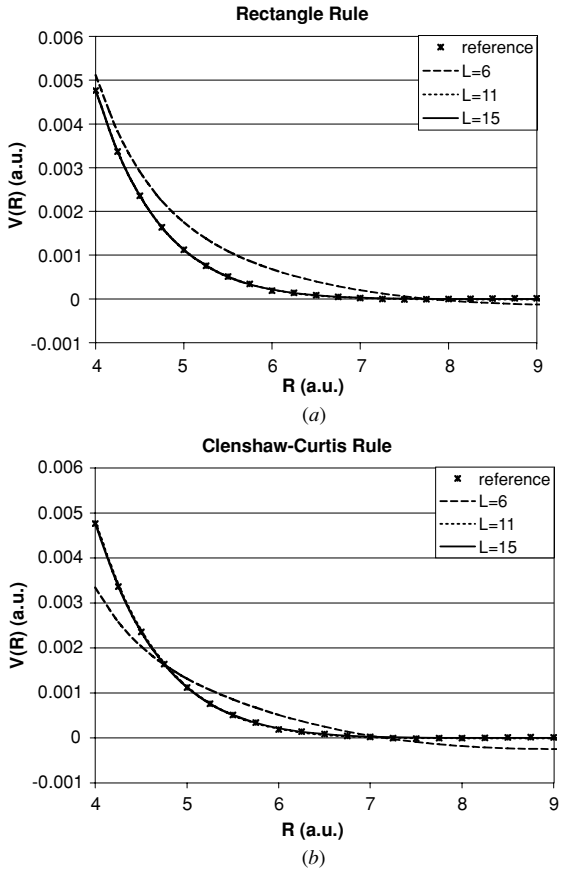

Figure 5. Smolyak formulae of various orders, L, are used to construct the potential energy of interaction for the H_2 molecule from applying the Thomas–Fermi–Dirac–McWeeny Gordon–Kim model to the Constans–Carbó atomic density fits. (*a*) Rectangle rule. (*b*) Clenshaw–Curtis rule. The reference data were obtained using third-party software (*Mathcad*).

In figure 5 we compare our results for the H_2 molecule to the values we obtained using third-party software (*Mathcad*, with integration tolerance TOL $= 10^{-8}$ and the default Romberg integration algorithm). As the order of integration increases, our integration method converges rapidly. It should be noted that the Gordon–Kim model fails to describe the substantial electron-density rearrangement that accompanies chemical binding in H_2, and so this interaction energy curve is not qualitatively correct. Our interest in this model is based primarily on its relevance for developing next-generation molecular mechanics force fields, where models similar to Gordon–Kim can be used to model the 'repulsive wall' on the potential energy curve that prevents atoms from coming too close together [58–61].

To evaluate the convergence of our methods in more detail, we engaged in a detailed study of the interaction energy expression for the Neon dimer, Ne_2. Some of the results from that study are shown in figure 6, where the convergence of the total interaction energy and each of its non-additive components are plotted. In figure 6, we plot the approximate 'number of digits of accuracy' in the formula, which we define through

$$\text{digits} = -\log_{10}\left(\frac{Q_L - Q_\infty}{Q_\infty}\right). \tag{29}$$

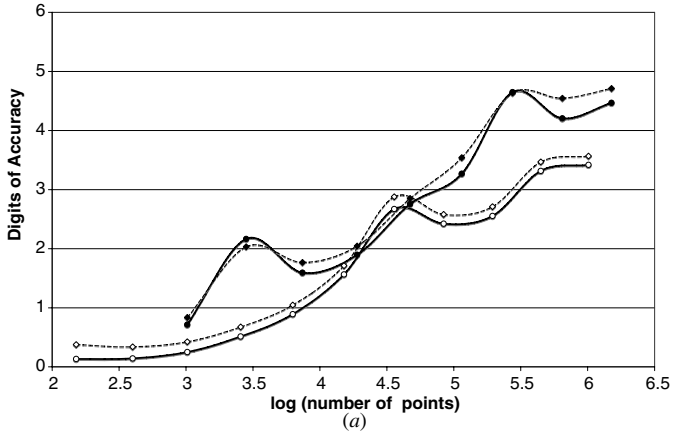

(*a*)

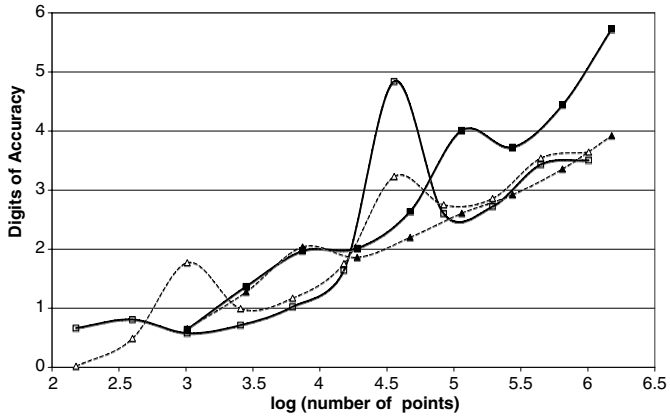

(*b*)

Figure 6. The number of digits of accuracy when Smolyak grids of various orders are used to evaluate the Thomas–Fermi–Dirac–McWeeny Gordon–Kim model of the Ne_2 interaction potential using the Constans–Carbó atomic density fits. The number of digits of accuracy (see equation (29) and the surrounding discussion) is plotted versus $\log_{10}$(number of grid points). Results for both the rectangle rule (closed symbols) and the Clenshaw–Curtis formula (open symbols) are reported. (*a*) Results for the total interaction potential (—●—) and the non-additive kinetic energy (—♦—). (*b*) Results for the non-additive exchange energy (—■—) and the non-additive correlation energy (—▲—).

Here, Q_L denotes the result from the integration formulae of order L and Q_∞ denotes the infinite-order limit. Since Q_∞ cannot be computed explicitly, we replaced this value with the result from the highest-order calculation we performed, $Q_{L_{\max}}$. Especially at low orders, the resulting plots provide a faithful representation of the rate of convergence with increasing number of points in the integration grid. Examining figure 6 in more detail, one observes that the rectangle rule typically performs better than the Clenshaw–Curtis rule, although the difference in performance is usually not as dramatic as it was for the simple Gaussian test function. The rectangle rule converges more rapidly for the exchange energy than it does for the kinetic energy, which is not surprising since $\rho^{4/3}(\mathbf{r})$ resembles the promolecular density used to construct the grid more closely than $\rho^{5/3}(\mathbf{r})$. The correlation energy component converges most slowly, which indicates that its relatively complicated functional form does not mimic the promolecular density very strongly. All of these results reinforce the expectation

that our integration technique will be most accurate when the weight function, $P(\mathbf{R})$, used to transform the grid strongly resembles the integrand of interest.

The largest component of the total interaction energy expression is the kinetic energy component. Thus, it is unsurprising that the error in the total interaction energy is dominated by the error in the non-additive kinetic energy. Iyengar *et al* also noted that very large integration grids are needed to accurately integrate kinetic energy functionals [62].

Note that the convergence in figure 6 is sometimes not monotone: smaller grids sometimes giving higher accuracy than larger grids. (There is a particular large oscillation in the convergence of the non-additive exchange energy using the Clenshaw–Curtis grid (cf figure 6(*b*)). Similar, but smaller, oscillations can be seen in figures 3 and 4.) These oscillations occur because the convergence of this sequence of numerical cubatures is not monotone. As the numerical integration result changes from greater than the true answer to less than the true answer, sometimes one is fortunate enough to find a relatively small integration grid that gives exceptionally high accuracy.

It should be stressed that the Gordon–Kim model represents a very strenuous test of our grids. For example, the non-additive kinetic energy is 400 times smaller than the kinetic energy of the promolecule, so obtaining four digits of accuracy in the non-additive kinetic energy requires *seven* digits of accuracy in the kinetic energy of the promolecule and the kinetic energy of the atoms.

3.3. The Gaussian model for the exchange energy

The favorable results for molecular interaction energies suggest that transformed Smolyak grids are more generally applicable, particularly in the context of density-functional theory. Here we will consider an application to a six-dimensional 'kernel-type' approximation to the exchange energy density functional.

Kernel-type density functionals allow us to write the exchange-correlation energy in terms of the exchange-correlation hole, and thus facilitate the direct probabilistic interpretation of exchange and correlation effects. Such functionals have a long and distinguished history, dating back to the weighted density approximation [63–69]. Progress has been impeded by the computational cost of performing six-dimensional integrals but, despite the cost, there has been a recent resurgence of interest in kernel-type functionals. Part of that interest is based on the explicit nonlocality of kernel-type functionals, which make it possible to model systems where the exchange-correlation hole is spatially delocalized [70, 71]. This seems to be particularly important for describing dispersion forces [72–76]. There is also interest stemming from the closely related pair-density functional theory, in which the exchange-correlation hole and the electron density are the fundamental variational parameters [77–82].

It is difficult to test whether the transformed Smolyak grids can be applied to this problem because of the absence of accurate numerical data to compare to. However, the six-dimensional Gaussian-kernel model of Lee and Parr is equivalent to a three-dimensional model [83]. Therefore, we can ascertain the accuracy of our numerical integration procedure by comparing the results we obtain from

$$E_x^{\mathrm{LP}}[\rho] = \frac{-1}{2}\iint \rho^2\left(\frac{\mathbf{r}+\mathbf{r}'}{2}\right)\exp\left(-\frac{\pi|\mathbf{r}-\mathbf{r}'|^2}{2^{2/3}\rho^{2/3}\left(\frac{\mathbf{r}+\mathbf{r}'}{2}\right)}\right)\times\frac{1}{|\mathbf{r}-\mathbf{r}'|}\,\mathrm{d}\mathbf{r}\,\mathrm{d}\mathbf{r}' \tag{30}$$

with the results of the Dirac-type exchange energy functional

$$E_x^{\mathrm{LP}}[\rho,0] = -2^{-1/3}\int \rho^{4/3}(\mathbf{r})\,\mathrm{d}\mathbf{r}. \tag{31}$$

Equation (31) is obtained from equation (30) by integrating over the interelectronic coordinate, $\mathbf{r} - \mathbf{r}'$.

The values of the three-dimensional integral (31) may be inferred from the results obtained from the Gordon–Kim model. (Compare equations (25) and (31).) To evaluate the six-dimensional integral (30), we choose the weight to be the product of the promolecular densities, $P(\mathbf{r}, \mathbf{r}') = \rho_{\text{pro}}(\mathbf{r})\rho_{\text{pro}}(\mathbf{r}')$. A disadvantage of this symmetric form is that points where $\mathbf{r} = \mathbf{r}'$ occur in our integration grid; this causes problems because the integrand in equation (30) is singular at these points. This can be circumvented by decomposing the functional into short-range and long-range pieces,

$$E_x^{\text{LP}}[\rho] = E_x^{\text{LP-SR}}[\rho] + E_x^{\text{LP-LR}}[\rho]. \tag{32}$$

The short-range and long-range pieces are defined using the complimentary error function and the error function, respectively:

$$E_x^{\text{LP-SR}}[\rho, \mu] = \frac{-1}{2} \iint \rho^2 \left(\frac{\mathbf{r}+\mathbf{r}'}{2}\right) \exp\left(-\frac{\pi|\mathbf{r}-\mathbf{r}'|^2}{2^{2/3}\rho^{-2/3}\left(\frac{\mathbf{r}+\mathbf{r}'}{2}\right)}\right) \times \frac{\operatorname{erfc}(\mu|\mathbf{r}-\mathbf{r}'|)}{|\mathbf{r}-\mathbf{r}'|}\, \mathrm{d}\mathbf{r}\, \mathrm{d}\mathbf{r}', \tag{33}$$

$$E_x^{\text{LP-LR}}[\rho, \mu] = \frac{-1}{2} \iint \rho^2 \left(\frac{\mathbf{r}+\mathbf{r}'}{2}\right) \exp\left(-\frac{\pi|\mathbf{r}-\mathbf{r}'|^2}{2^{2/3}\rho^{-2/3}\left(\frac{\mathbf{r}+\mathbf{r}'}{2}\right)}\right) \times \frac{\operatorname{erf}(\mu|\mathbf{r}-\mathbf{r}'|)}{|\mathbf{r}-r'|}\, \mathrm{d}\mathbf{r}\, \mathrm{d}\mathbf{r}'. \tag{34}$$

A three-dimensional density-functional model is achieved for the singular 'short-range' functional using the time-honored, but tedious and difficult, approach [84–86]. The integrand of the 'long-range' functional is not singular and can be evaluated numerically. Figure 7 shows results for the Neon dimer obtained using the Smolyak-rectangle rule of various orders, L. Note that as μ increases, the value of the integrand approaches the accurate value computed from equation (31). For the higher values of μ considered here, the integrand is very strongly peaked where $\mathbf{r} \approx \mathbf{r}'$; this is why the order of integration needed to obtain converged results increases rapidly as μ increases. Fortunately, it is possible to develop very good short-range functionals, so the value of μ can remain quite small.

4. Summary

We have developed an efficient method for general multi-dimensional integrals with respect to arbitrary weight functions (i.e., integrals with the form of equation (1)). Our approach uses the Smolyak method to first construct cubature grids on the cube, $[0, 1]^d$ (cf equation (10)) and then uses the conditional distribution transformation to generate integration grids in real space with respect to any given weight function (cf equation (13)). Our numerical results converge rapidly to the correct answer as the order of integration grids increases. We applied the grids to the Gordon–Kim model for atomic interactions [47] and the Lee–Parr Gaussian model for the exchange energy [83].

These calculations can be seen as 'proof of principle' studies for two areas where we see this method having broad applicability. The Gordon–Kim calculations are directly relevant to the field of frozen-density embedding, where 'improved' Gordon–Kim models are used to model non-covalent interactions between solutes and solvents, metals and ligands, etc [87–91]. More generally, the quality of our results for the Gordon–Kim model indicates that this method will be generally useful for the evaluation of density functionals. It would certainly be interesting, for example, to study more sophisticated kinetic energy functionals. It is of

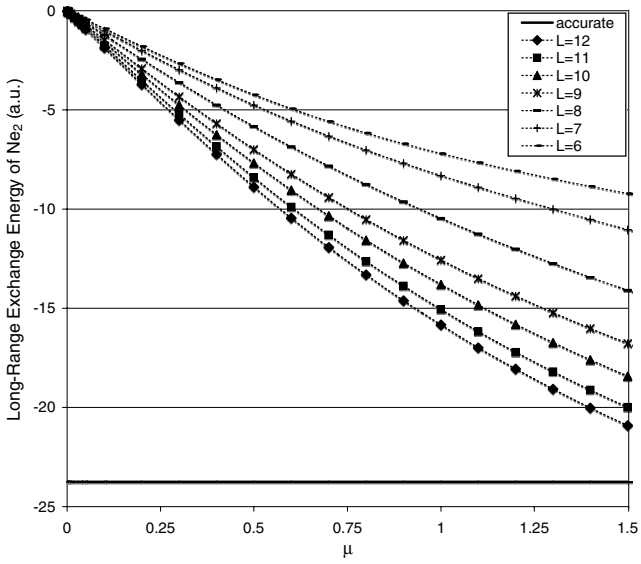

Figure 7. The long-range contribution to the exchange energy, equation (34), for the Neon dimer with internuclear separation 2.5 au. is computed using the Smolyak-rectangle rule integration of various orders, L, for different values of the range separation parameter, μ. Atomic units are used.

greater direct interest, however, to consider using the transformed Smolyak grids as the default integration method for evaluating the exchange-correlation energies and exchange-correlation potentials in Kohn–Sham density-functional theory. We performed such studies and obtained excellent results [34].

The application to nonlocal, kernel-type, exchange-correlation functionals shows that this integration method may be profitably used for six-dimensional integrals. While nonlocal exchange-correlation functionals are indubitably of great current interest [63–69], the same methods are relevant to 'generalized' density-functional theories [92, 93], most notably the pair-density functional theory [77–82] and the first-order density matrix functional theory [94–96]. We are currently working on applications in both nonlocal exchange-correlation density functionals and pair-density functional theory.

At the mathematical level, we are examining methods for improving the efficiency of our numerical integration grids. For example, would it be helpful to use the 'promolecular' exchange-correlation energy density (instead of the promolecular electron density) as the weight function for the transformation? How well do other sparse-grid methods work? Are there better one-dimensional formulae than the Clenshaw–Curtis and the rectangle rule? Answering these questions will help us develop improved numerical integration grids. Such grids (a) have few points, (b) can be rapidly constructed and (c) give very accurate results for the integrals that arise in electronic structure modeling.

We also intend to extend this approach to other problems in molecular electronic structure theory. We have already shown that the transformed Smolyak grids can be used to evaluate the exchange-correlation matrix elements that arise in Kohn–Sham DFT calculations [34]. One can also imagine using the transformed Smolyak grids as the basis for a truly basis-set-free approach to molecular electronic structure. Such a method requires combining the integration methods explored in this paper with differentiation techniques for the transformed Smolyak grids [40, 41] and grid-based solvers for second-order differential equations [27, 32, 33, 97, 98] or grid-based techniques for variational minimization of the energy.

Acknowledgments

Juan I Rodriguez and James S M Anderson acknowledge graduate fellowships from 'Consejo Nacional de Ciencia y Tecnología-México' and NSERC, respectively. Jordan W Thomson acknowledges an 'Undergraduate Student Research Award' from NSERC. Paul W Ayers acknowledges support from NSERC, the Canada Research Chairs and Sharcnet.

References

[1] Kato T 1957 *Commun. Pure Appl. Math.* **10** 151–77
[2] Steiner E 1963 *J. Chem. Phys.* **39** 2365–6
[3] Bene E and Nagy A 2000 *J. Mol. Struct.—Theochem.* **501** 107–13
[4] Nagy A and Sen K D 2000 *Chem. Phys. Lett.* **332** 154–8
[5] Nagy A and Sen K D 2000 *J. Phys.* B **33** 1745–51
[6] Nagy A and Sen K D 2001 *J. Chem. Phys.* **115** 6300–8
[7] Ayers P W 2000 *Proc. Natl Acad. Sci.* **97** 1959–64
[8] Gautschi W 1994 *ACM Trans. Math. Softw.* **20** 21–62
[9] Gautschi W 1996 *Acta Numer.* **5** 45–119
[10] Gautschi W 1998 *ACM Trans. Math. Softw.* **24** 355–7
[11] Gautschi W 2004 *Orthogonal Polynomials: Computation and Approximation* (New York: Oxford University Press)
[12] Rees D and Hall G G 2005 *Int. J. Quantum Chem.* **102** 19–30
[13] Hall G G and Rees D 2007 *Int. J. Quantum Chem.* **107** 845–57
[14] Cools R and Rabinowitz P 1993 *J. Comput. Appl. Math.* **48** 309–26
[15] Cools R 1999 *J. Comput. Appl. Math.* **112** 21–7
[16] Cools R 2003 *J. Complexity* **19** 445–53
[17] Smolyak S A 1963 *Dokl. Akad. Nauk* **4** 240–3
[18] Traub J F and Wozniakowski H 1992 *Bull. AMS* **26** 29–52
[19] Traub J F and Werschulz A G 1998 *Complexity and Information* (Cambridge: Cambridge University Press)
[20] Temme N M 1996 *Special Functions: an Introduction to the Classical Functions of Mathematical Physics* (New York: Wiley)
[21] Weideman J A C and Trefethen L N 2007 *Numer. Math.* **107** 707–27
[22] Trefethen L N 2008 *SIAM Rev.* **50** 67–87
[23] Murray C W, Handy N C and Laming G J 1993 *Mol. Phys.* **78** 997–1014
[24] Xu Y 1994 *Common Zeros of Polynomials in Several Variables and Higher Dimensional Quadrature* (New York: Wiley)
[25] Wasilkowski G W and Wozniakowski H 1995 *J. Complexity* **11** 1–56
[26] Novak E and Ritter K 1999 *Constructive Approx.* **15** 499–522
[27] Bungartz H J and Griebel M 1999 *J. Complexity* **15** 167–99
[28] Griebel M and Knapek S 2000 *Constructive Approx.* **16** 525–40
[29] Yserentant H 2004 *Numer. Math.* **98** 731–59
[30] Yserentant H 2005 *Numer. Math.* **101** 381–9
[31] Yserentant H 2007 *Numer. Math.* **105** 659–90
[32] Garcke J and Griebel M 2000 *J. Comput. Phys.* **165** 694–716
[33] Griebel M and Hamaekers J 2007 *Esaim-Math. Modelling Numer. Anal.* **41** 215–47
[34] Rodríguez J I, Thompson D C, Ayers P W and Köster A M 2008 *J. Chem. Phys.* **128** 224103
[35] Bungartz H and Griebel M 2001 *Acta Numer.* **13** 147–269
[36] Novak E and Ritter K 1996 *Numer. Math.* **75** 79–97
[37] Cools R, Novak E and Ritter K 1999 *Computing* **62** 147–62
[38] Devroye L 1986 *Non-uniform Random Variate Generation* (New York: Springer)
[39] Perez-Jorda J M 1989 *Eur. J. Phys.* **10** 224–34
[40] Thompson D C and Ayers P W 2006 *Int. J. Quantum Chem.* **106** 787–94
[41] Anderson J S M, Rodriguez J I, Thompson D C and Ayers P W 2007 *Quantum Chemistry Research Trends* (New York: Nova)
[42] Perez-Jorda J M 1995 *Phys. Rev.* A **52** 2778–85
[43] McMurchie L E and Davidson E R 1978 *J. Comput. Phys.* **26** 218–31
[44] Boys S F 1950 *Proc. R. Soc. Lond.* A **200** 542–54

[45] Constans P and Carbó R 1995 *J. Chem. Inform. Comput. Sci.* **35** 1046–53
[46] Hirshfeld F L 1977 *Theor. Chim. Acta* **44** 129–38
[47] Gordon R G and Kim Y S 1972 *J. Chem. Phys.* **56** 3122–33
[48] Thomas L H 1927 *Proc. Camb. Phil. Soc.* **23** 542–8
[49] Fermi E 1928 *Z. Phys.* **48** 73–9
[50] McWeeny R 1976 *New World Quantum Chem., Proc. Int. Congr.* vol 2 pp 3–31
[51] Wigner E 1934 *Phys. Rev.* **46** 1002–11
[52] Dirac P A M 1930 *Proc. Camb. Phil. Soc.* **26** 376–85
[53] Slater J C 1951 *Phys. Rev.* **81** 385–90
[54] Kohn W and Sham L J 1965 *Phys. Rev.* **140** A1133–8
[55] Rae A I M 1973 *Chem. Phys. Lett.* **18** 574–7
[56] Rae A I M 1975 *Mol. Phys.* **29** 467–83
[57] Perdew J P and Zunger A 1981 *Phys. Rev.* B **23** 5048–79
[58] Cisneros G A, Piquemal J P and Darden T A 2005 *J. Chem. Phys.* **123** 044109
[59] Piquemal J P, Perera L, Cisneros G A, Ren P Y, Pedersen L G and Darden T A 2006 *J. Chem. Phys.* **125** 054511
[60] Piquemal J P, Cisneros G A, Reinhardt P, Gresh N and Darden T A 2006 *J. Chem. Phys.* **124** 104101
[61] Cisneros G A, Piquemal J P and Darden T A 2006 *J. Chem. Phys.* **125** 184101
[62] Iyengar S S, Ernzerhof M, Maximoff S N and Scuseria G E 2001 *Phys. Rev.* A **63** (art-052508)
[63] Gunnarsson O, Jonson M and Lundqvist B I 1976 *Phys. Lett.* A **59** 177–9
[64] Alonso J A and Girifalco L A 1977 *Solid State Commun.* **24** 135–8
[65] Gunnarsson O, Jonson M and Lundqvist B I 1977 *Solid State Commun.* **24** 765–8
[66] Alonso J A and Girifalco L A 1978 *Phys. Rev.* B **17** 3735–43
[67] Gunnarsson O and Jones R O 1980 *Phys. Scr.* **21** 394–401
[68] Pedroza A C 1986 *Phys. Rev.* A **33** 804–13
[69] Amovilli C and March N H 2007 *Phys. Rev.* B **76** 195104
[70] Gritsenko O V, Ensing B, Schipper P R T and Baerends E J 2000 *J. Phys. Chem.* A **104** 8558–65
[71] Zhang Y and Yang W 1998 *J. Chem. Phys.* **109** 2604–8
[72] Dion M, Rydberg H, Schroder E, Langreth D C and Lundqvist B I 2004 *Phys. Rev. Lett.* **92** 246401
[73] Thonhauser T, Puzder A and Langreth D C 2006 *J. Chem. Phys.* **124** 164106
[74] Puzder A, Dion M and Langreth D C 2006 *J. Chem. Phys.* **124** 164105
[75] Kleis J, Lundqvist B I, Langreth D C and Schoder E 2007 *Phys. Rev.* B **76** 100201
[76] Thonhauser T, Cooper V R, Li S, Puzder A, Hyldgaard P and Langreth D C 2007 *Phys. Rev.* B **76** 125112
[77] Ziesche P 1994 *Phys. Lett.* A **195** 213–20
[78] Ziesche P 1996 *Int. J. Quantum Chem.* **60** 1361–74
[79] Nagy A 2002 *Phys. Rev.* A **66** 022505
[80] Nagy A and Amovilli C 2004 *J. Chem. Phys.* **121** 6640–8
[81] Ayers P W 2005 *J. Math. Phys.* **46** 062107
[82] Ayers P W, Golden S and Levy M 2006 *J. Chem. Phys.* **124** 054101
[83] Lee C and Parr R G 1987 *Phys. Rev.* A **35** 2377–83
[84] Toulouse J, Gori-Giorgi P and Savin A 2005 *Theor. Chem. Acc.* **114** 305–8
[85] Toulouse J, Colonna F and Savin A 2005 *J. Chem. Phys.* **122**
[86] Toulouse J, Savin A and Flad H J 2004 *Int. J. Quantum Chem.* **100** 1047–56
[87] Cortona P 1991 *Phys. Rev.* B **44** 8454–8
[88] Wesolowski T A and Warshel A 1993 *J. Phys. Chem.* **97** 8050–3
[89] Vaidehi N, Wesolowski T A and Warshel A 1992 *J. Chem. Phys.* **97** 4264–71
[90] Wesolowski T A and Leszczynski J 2006 *Computational Chemistry: Reviews of Current Trends* (Singapore: World Scientific) pp 1–82
[91] Govind N, Wang Y A and Carter E A 1999 *J. Chem. Phys.* **110** 7677–88
[92] Ayers P W 2006 *Phys. Rev.* A **74** 042502
[93] Ayers P W and Levy M 2005 *J. Chem. Sci.* **117** 507–14
[94] Levy M 1979 *Proc. Natl Acad. Sci.* **76** 6062–5
[95] Gilbert T L 1975 *Phys. Rev.* B **12** 2111–20
[96] Donnelly R A and Parr R G 1978 *J. Chem. Phys.* **69** 4431–9
[97] Griebel M 1998 *Computing* **61** 151–79
[98] Garcke J and Griebel M 2000 *J. Comput. Phys.* **165** 694–716